

# Deciphering the Mesodermal Potency of Porcine Skin-Derived Progenitors (SKP) by Microarray Analysis

Ming-Tao Zhao,<sup>1,2</sup> Kristin M. Whitworth,<sup>1</sup> Xia Zhang,<sup>1</sup> Jianguo Zhao,<sup>1</sup> Yi-Liang Miao,<sup>3</sup>  
Yong Zhang,<sup>2</sup> and Randall S. Prather<sup>1</sup>

## Abstract

Skin stem cells have an essential role in maintaining tissue homeostasis by dynamically replenishing those constantly lost during tissue turnover or following injury. Multipotent skin derived progenitors (SKP) can generate both neural and mesodermal progeny, representing neural crest-derived progenitors during embryogenesis through adulthood. SKP cells develop into spheres in suspension and can differentiate into fibroblast-like cells (SFC) in adhesive culture with serum. Concomitantly they gradually lose the neural potential but retain certain mesodermal potential. However, little is known about the molecular mechanism of the transition of SKP spheres into SFC *in vitro*. Here we characterized the transcriptional profiles of porcine SKP spheres and SFC by microarray analysis. We found 305 upregulated and 96 downregulated genes, respectively. The downregulated genes are mostly involved in intrinsic programs like the *Dicer* pathway and asymmetric cell division, whereas upregulated genes are likely to participate in extrinsic signaling pathways such as ErbB signaling, MAPK signaling, ECM-receptor reaction, Wnt signaling, cell communication, and tumor growth factor (TGF)- $\beta$  signaling pathways. These intrinsic programs and extrinsic signaling pathways collaborate to mediate the transcription-state transition between SKP spheres and SFC. We speculate that these potential signaling pathways may play an important role in regulating the cell fate transition between SKP spheres and SFC *in vitro*.

## Introduction

**S**KIN-DERIVED PROGENITOR (SKP) CELLS from mammalian dermis can differentiate into cells of both neural and mesodermal lineages, such as neurons, glia, smooth muscle cells, and adipocytes (Dyce et al., 2004; Fernandes et al., 2004; Toma et al., 2001; Zhao et al., 2009). SKP cells that exhibit similar characteristics of embryonic neural crest stem cells can develop into neurosphere-like morphology in suspension culture, and can be passaged for 1 year without losing their multiple differentiation potential (Fernandes et al., 2004; Toma et al., 2001). However, SKP spheres initiate differentiation when they attach onto the culture dishes by serum. After the attachment, they develop into a fibroblast-like morphology which is similar to that of multipotent mesenchymal stem cells (Pittenger et al., 1999). During this process SKP cells gradually lose their neural potency but retain their mesodermal potency and can be induced into smooth muscle cells and adipocytes (Fernandes et al., 2008; Zhao et al., 2009). Comparatively, mesenchymal stem cells (MSCs) can differentiate

into various cell types *in vitro* and *in vivo*, including osteoblasts, chondrocytes, myocytes, and adipocytes (Pittenger et al., 1999); although the pluripotency of MSCs has still been controversial (Jiang et al., 2002; Terada et al., 2002; Ying et al., 2002). It has been reported that dermal skin-derived fibroblasts have the capacity to differentiate into osteogenic, chondrogenic, myogenic, and adipogenic lineages, showing characteristics similar to MSC (Crigler et al., 2007; Lorenz et al., 2008). In addition, several other multipotent dermis-derived stem cells have been identified by using different culture systems, implying the prospective therapeutic applications because skin is easily accessible for autologous transplantation (Bartsch et al., 2005; Chen et al., 2007). These findings support a view that multipotent stem cells can be isolated from dermal skin, although they display different characteristics in response to various extrinsic stimuli.

There is still a debate about the plasticity of adult stem cells (Wagers and Weissman, 2004). The extrinsic environment plays an important role in defining the stem cell niches during embryonic development, whereas intrinsic programs that

<sup>1</sup>Division of Animal Sciences, University of Missouri, Columbia, Missouri.

<sup>2</sup>Institute of Biotechnology, Northwest A&F University, Yangling, Shaanxi, People's Republic of China.

<sup>3</sup>Department of Veterinary Pathobiology, University of Missouri, Columbia, Missouri.

determine the transcriptional state of stem cells may be adjusted to lineage commitment in response to extrinsic signaling (Albert and Peters, 2009; Arnold and Robertson, 2009). To some extent, *in vitro* culture conditions sometimes alter the behavior of stem cells by modifying their fates and even their developmental potentials (Joseph and Morrison, 2005). This idea has been further confirmed by reprogramming differentiated cells back into a pluripotent stem cell state either by ectopic expression of specific transcription factors or using recombinant proteins *in vitro* (Kim et al., 2009a; Takahashi and Yamanaka, 2006; Zhou et al., 2009). Thus, it seems as if the extrinsic stimulus would alter the developmental potential of SKP cells *in vitro* through a shift of transcriptional states.

Genome-wide transcriptional profiling has become a routine assay with the development of microarray technology (Hoheisel, 2006). Transcriptional profiling of multipotent stem/progenitor cells has been extensively investigated on embryonic stem cells (Ivanova et al., 2002; Ramalho-Santos et al., 2002), neural stem cells (Maisel et al., 2007; Shin et al., 2007), hematopoietic stem cells (Kiel et al., 2005; Terskikh et al., 2003), MSCs (Song et al., 2006; Wagner et al., 2005), and epithelial stem cells (Tumbar et al., 2004) by microarray technology. Nevertheless, the transcriptional program of multipotent skin-derived stem cells such as SKP cells has yet to be determined. Moreover, the comparison of the molecular signatures between SKP and other skin-derived progenitor cells remains an open question. Hence, the aim of this study is to compare the transcriptional programs between SKP spheres and SKP-derived fibroblast-like cells (SFC) by microarray analysis. We assume that the individual transcriptional states may be established in specific microenvironment by SKP spheres and SFC, which can be regulated and maintained through divergent signaling pathways. This would help to explain the molecular mechanisms of neural and mesodermal potential of SKP cells, thus accelerating the therapeutic application of skin-derived stem cells.

## Methods and Materials

Animal use and care have been reviewed and approved by the Animal Care and Use Committee (ACUC) at University of Missouri–Columbia.

### Cell isolation and cultures

Chemicals and components were purchased from Sigma (St. Louis, MO, USA) unless indicated otherwise.

The isolation of porcine SKP spheres was described elsewhere (Zhao et al., 2009). Briefly, back skin tissue was peeled off from day 40–50 pCAG-EGFP transgenic porcine fetuses in a sterile hood (Whitworth et al., 2009). The tissues were washed with D-PBS (Invitrogen, Carlsbad, CA, USA) three times and chopped up into small pieces. Then the tissue was digested by 0.1% trypsin for 20–40 min at 37°C. Afterward, 1 mL of 0.1% DNase I was added and incubated for 1 min at room temperature (RT). The enzymatic activity of trypsin was counteracted with neutralization solution [DMEM/F12 (1:1, Invitrogen) + 10% fetal bovine serum (FBS)] (Hyclone, Logan, UT, USA) and the cells were washed three times with DMEM/F12 medium. The cells were subsequently dissociated and poured through a 40- $\mu$ m strainer (BD Biosciences, Franklin Lakes, NJ, USA). The dissociated cells were collected by centrifugation and resuspended with standard

culture medium containing DMEM/F12 (1:1), B27 (50 $\times$ , Invitrogen), 20 ng/mL EGF and 40 ng/mL bFGF. After 3 d culture in suspension dishes (Sarstedt, Newton, NC, USA), an appropriate volume of culture medium with 2 $\times$  growth factor and supplements was added to complement the depletion. The SKP spheres appeared in 5–7 days and were harvested for RNA isolation or stored in liquid nitrogen.

For SFC derivation, SKP spheres were collected and resuspended by induction medium [DEME (Invitrogen) + 15% FBS + 20 ng/mL EGF] and plated onto a 24-well cell culture cluster (Corning Incorporated, Corning, NY, USA). The SFCs were cultured for 3 days and recovered by 0.05% trypsin/EDTA (Invitrogen). The trypsin was neutralized by 3 $\times$  volumes of induction medium and the cells were collected. The SKP-derived fibroblast-like cells were immediately frozen for RNA isolation or stored in liquid nitrogen.

### Immunocytochemistry

Cell cultures were fixed by 4% paraformaldehyde and then permeabilized with 0.1% Triton X-100 for 20 min. The fixed cells were blocked with PBS/10% FBS for 2 h and subsequently incubated with primary antibody overnight at 4°C. After washing with PBS/10% FBS, they were incubated with secondary antibody for 1 h at RT. Finally they were incubated with Hoechst 33342 for 15 min. A parallel culture only with secondary antibody was employed as a negative control and culture without any antibody was used as a blank control. Primary antibodies were monoclonal antifibronectin (Abcam, Cambridge, MA, USA; 1:200), monoclonal anti-vimentin (Abcam, 1:200), monoclonal anti-GFAP (Sigma, 1:250), monoclonal antitubulin  $\beta$ -III (Sigma, 1:250), monoclonal anti-NFM (Abcam, 1:100), and monoclonal anti-p75NTR (Abcam, 1:100). Secondary antibodies were Alexa Fluor® 594 goat antimouse IgG (H + L) (Invitrogen, 1:500). The images were captured by DS Camera Control Unit DS-U2 (Nikon, Melville, NY, USA) and processed by using the NIS-Elements imaging software (Nikon). Each slide for immunocytochemistry was independently repeated three times.

### RNA isolation and amplification

Total RNA was extracted by using an AllPrep DNA/RNA mini kit (Qiagen, Valencia, CA, USA) and measured by a NanoDrop Spectrophotometer (Thermo Fisher Scientific Inc., Wilmington, DE, USA). The RNA amplification was performed by WT-Ovation Pico RNA amplification system (NuGEN, San Carlos, CA, USA) with the input of 5 ng of RNA. The amplified cDNA was purified by Micro Bio-Spin 30 Columns in RNase-Free Tris (Bio-Rad Laboratories, Hercules, CA, USA). The purified cDNA was aliquoted into 1  $\mu$ g per vial and stored at –80°C.

### Reference RNA (Ref RNA) preparation

The porcine Ref RNA was created by isolating total RNA from a large representation of nonreproductive and reproductive tissues across different developmental stages (Whitworth et al., 2005). Ref RNA was reverse transcribed by SuperScript III First-Strand Synthesis System (Invitrogen) and purified by Micro Bio-Spin 30 Columns in RNase-Free Tris. The purified Ref cDNA was aliquoted and stored at –80°C.

### cDNA microarray preparation

The cDNA microarray platform was established at the University of Missouri–Columbia (Agca et al., 2006; Green et al., 2006; Whitworth et al., 2004, 2005). The general information of EST clones can be browsed at <http://genome.mnet.missouri.edu/Swine/>.

### Labeling and hybridization

The starting amount of purified Ref cDNA or amplified cDNA sample was 1  $\mu$ g. The amplified cDNA samples were labeled with Cy5 (ULYSIS Alexa Fluor 647 Nucleic Acid Labeling Kits, Invitrogen) and Ref cDNA was labeled with Cy3 (ULYSIS Alexa Fluor 546 Nucleic Acid Labeling Kits, Invitrogen). After labeling and purification, NanoDrop readings were processed to calculate the degree of labeling (DoL, <http://www.kreatech.com/Default.aspx?tabid=121>) and to validate that labeling efficiency was within the recommended range of 1–3.6%. Then the Cy5-labeled samples and Cy3-labeled Ref cDNA were combined together and dried in a CentriVap Concentrator system. The labeled cDNA were resuspended with hybridization buffer (50% formamide, 0.1% SDS and 5 $\times$ SSC) and blocked with 1  $\mu$ L of 20 ng/ $\mu$ L polyA (20 mers) to prevent hybridization to the 3' end of the ESTs. Then they were denatured at 95°C for 3 min and cooled at RT. The labeled cDNA was subsequently applied from one end to the arrays and incubated at 42°C for 16 h with gentle shaking.

### Microarray replicates

Each biological replicate consisted of RNA from 1 $\times$ 10<sup>5</sup> cells of SKP spheres or SFCs, which were derived from the

pools of two different fetuses either in the same litters or different litters. Each biological replicate was analyzed on two microarrays, resulting in three biological replicates and two technical replicates, that is, six microarray measurements.

### Wash and Scan arrays

After hybridization, the arrays were washed with washing solution I (2 $\times$ SSC/0.1% SDS) twice, washing solution II (0.1 $\times$ SSC/0.1% SDS) once and washing solution III (0.1 $\times$ SSC), each of which was kept on a shaker for 4 min covered with foil to avoid light. The slides were then shifted into 95% ethanol for a few seconds and centrifuged at 1500 rpm for 5 min. Subsequently the arrays were scanned by GenePix 4000B (Molecular Devices, Sunnyvale, CA, USA). The PMTs for wave length 532 and 653 were adjusted appropriately to ensure that the count ratio of Cy3 to Cy5 is 1.0. The images were visualized by GenePix Pro 4.1 (Molecular Devices) to assess the spot quality. The proper gene array list was loaded and poor-quality spots (smeared or saturated) were flagged manually. Then the raw data were generated as input for further analysis.

### Data analysis by GeneSpring GX 7.3.1

The general strategy for microarray data analysis is outlined in Figure 1. The raw data were uploaded into GeneSpring GX 7.3.1 (Agilent Technologies, Santa Clara, CA, USA). The spots were filtered to remove those whose raw intensities were close to background and not reliable. One-way analysis of variance (ANOVA) was performed by using a parametric test with variances not assumed equal (Welch *t*-test) and *p*-value cutoff of 0.05.

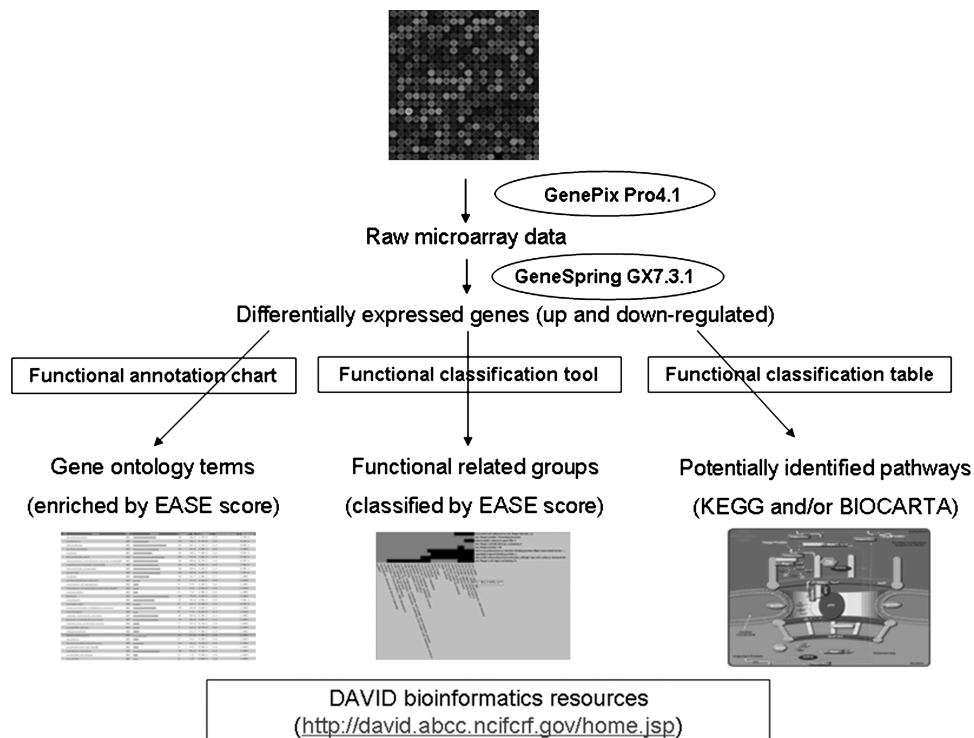


FIG. 1. The strategy used for microarray data analysis: finding potential pathways.

*Database for annotation, visualization and integrated discovery (DAVID) analysis*

The online DAVID (sixth version, 2008) was employed to perform functional annotation analysis (Dennis et al., 2003; Huang da et al., 2009). The upregulated and downregulated gene lists were submitted and converted into DAVID IDs. Subsequently the uploaded DAVID lists were subject to Functional Annotation Clustering, which uses fuzzy clustering by measuring the relationships among the annotation terms on the basis of the degree of their coassociation with genes within the user's list to cluster somewhat heterogeneous, yet highly similar annotation into functional annotation groups. A higher enriched score indicates that the gene members in the groups are involved in more important roles, which can be visualized by a 2D view tool. Gene Functional Classification Tool was used to group genes based on functional similarity, displaying with group enrichment scores according to overall EASE scores of all enriched annotation

terms. The Functional Annotation Chart shows the enriched gene ontology terms associated with input genes, which pass the threshold of EASE score ( $p \leq 0.05$ ). In addition, the related KEGG pathways or BIOCARTA pathways can be found in Functional Annotation Tables.

*Real-time qPCR validation*

Six genes were selected to verify the microarray data. The primers were synthesized by Integrated DNA Technologies (IDT, Skokie, IL, USA). Real-time qPCR was carried out by using Power SYBR Master Mix in ABI Prism 7500 real-time PCR system (Applied Biosystems, Carlsbad, CA, USA). The expression levels were normalized by a relative standard curve method. Gradient dilutions (1/10 $\times$ ) of Ref cDNA were used for creating standard curves. The housekeeping gene *GAPDH* was used as a calibrator gene. The real-time qPCR data were obtained from three independent biological replicates and two technical replicates and analyzed by one-way ANOVA.

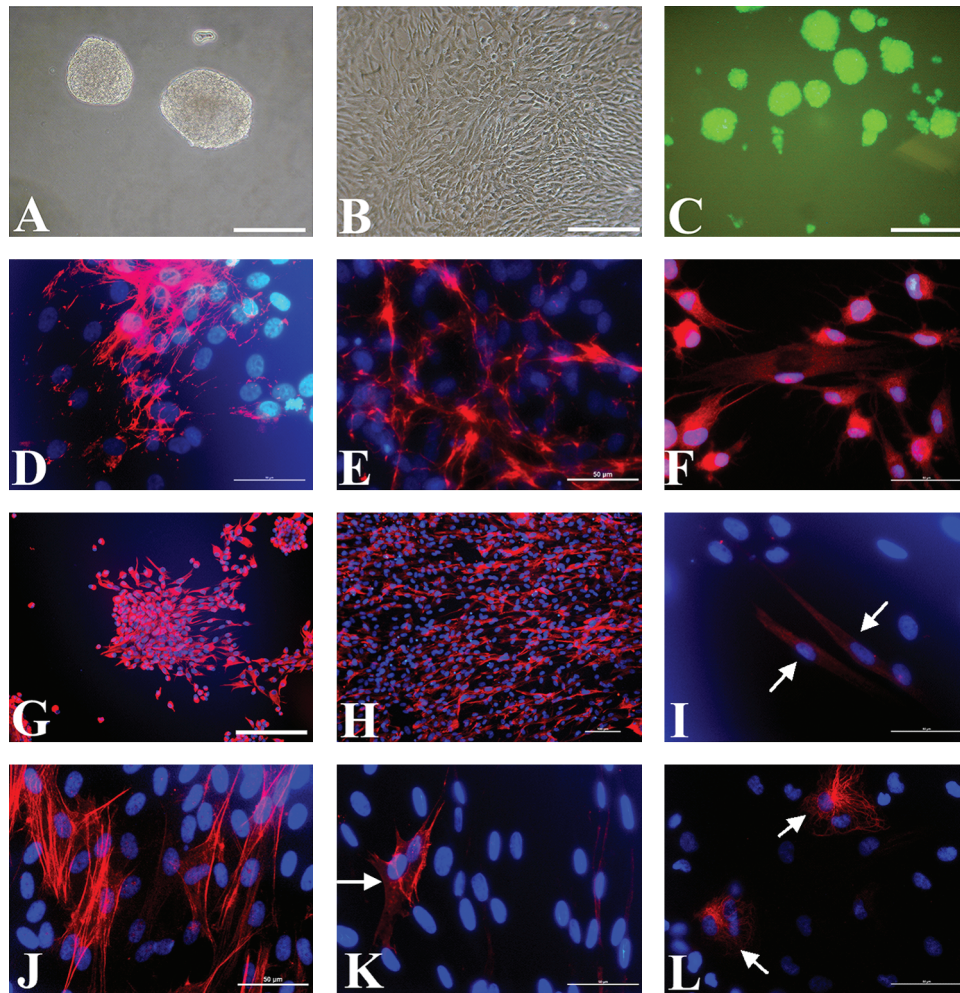


**FIG. 2.** Characterization of porcine SKP spheres and SFC cells *in vitro*. Typical SKP spheres (A) and SFC (B) under phase contrast, and EGFP SKP spheres under fluorescence (C) are shown. Both SKP spheres and SFC cells expressed fibronectin and vimentin: (D–E) the merged images of anti-fibronectin and Hoechst 33342 staining for SKP spheres (D) and SFC (E); (G–H) the overlay of antivimentin and Hoechst 33342 staining for SKP spheres (G) and SFC (H). The multiple-lineage differentiation of SKP spheres was shown (F, I, K, L). SKP sphere-derived progeny were immunostained with monoclonal antibodies against tubulin  $\beta$ -III (F), GFAP (I), SMA (K), NFM (L), and the nuclei were stained by Hoechst 33342. However, SMA positive cells (J) were also present in SFC cultures. Scale bars, 50  $\mu$ m (D–F, I–L); 100  $\mu$ m (H); 200  $\mu$ m (A–C, G).

## Results

### Characterization of porcine SKP spheres and SFC cells *in vitro*

The porcine SKP cells developed into sphere-like structure in suspension cultures (Fig. 2A and C), which is quite different from the colonies of keratinocytes on feeder cells (Rheinwald and Green, 1975). However, they attached onto the bottom and exhibited fibroblast-like morphology when exposed to serum and tissue culture treated dishes (Fig. 2B). Both porcine SKP spheres and SFC can express fibronectin and vimentin (Fig. 2D, E, G, and H) when measured by immunocytochemistry, similar to that of human adherent SKP cells (Toma et al., 2005) but distinct from that of rodent SKP cells (Toma et al., 2001). Smooth muscle actin (SMA) can be detected in SFC cultures (Fig. 2J) rather than SKP spheres, although SMA-positive cells appeared during the differentiation of SKP spheres (Fig. 2K). After differentiation, SKP spheres could generate tubulin  $\beta$ -III positive (Fig. 2F) cells, GFAP positive (Fig. 2I) cells, and neurofilament M (Fig. 2L) positive cells, indicating the neural potential of SKP cells *in vitro* (Zhao et al., 2009). However, these neural progeny did not appear in induced SFC cultures (data not shown). This suggests the loss of neural potential for SFC, which is inconsistent with neurogenic differentiation potency of human nestin negative vimentin positive dermal fibroblast clones (Chen et al., 2007).

Next we compared the marker gene expression between porcine SKP spheres and SFC. We observed a similar pattern of marker gene expression between the two (Fig. 3), such as embryonic stem (ES) cell marker *NANOG* (Chambers et al., 2007; Mitsui et al., 2003), *STAT3* (Niwa et al., 1998) and neural crest cell marker *TWIST1*, *SNAI2*, and *p75NTR* (Sauka-Spengler and Bronner-Fraser, 2008). Nevertheless, *SOX10* was exclusively expressed in SKP rather than in SFC, although *SOX10* mRNA signal was faint in SKP spheres (Kim et al., 2003). In addition, the expression of fibronectin and vimentin was confirmed by immunocytochemistry (Fig. 2D, E, G, and H). These results show similar marker gene expression patterns between SKP and SFC, but they display differential differentiation potential. Together, we demonstrate the neural and mesodermal potency of SKP spheres *in vitro*. During the transition between SKP spheres into SFC, neural potential is gradually lost but mesodermal potential is still retained in SFC.

### Functional annotation clustering of upregulated genes

Because SFC cells were derived from SKP, they should have the same genetic background with low transcriptional noise. We only used the signals with the intensity of 1500 to 60,000 in the raw and control data as determined by GeneSpring GX 7.3.1. Totally, there were 401 differentially expressed genes between SKP and SFC ( $p \leq 0.05$ ), of which 305 genes were upregulated compared with those expression levels of SKP. The upregulated gene lists were submitted and converted into 188 DAVID IDs. The gene ontology (GO) terms of upregulated genes are listed in Table 1 with a  $p$ -value cutoff 0.05. Most of upregulated genes have the terms of binding, cellular process, and metabolic process (Table 1). Furthermore, these genes were functionally clustered into 10 groups by enrichment scores (Table 2): cellular protein metabolic process (4.97), nucleotide binding (2.49), response to protein

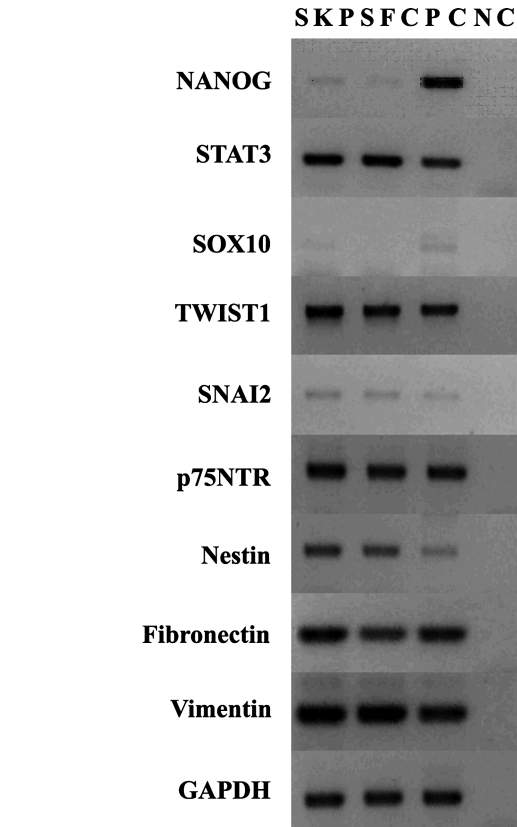


**FIG. 3.** Marker gene expression between SKP spheres and SFC. The Ref cDNA was used as the template for the positive control (PC), whereas no RT was used as the negative control (NC). The RT-PCR was replicated by three biological samples and only one was shown. The housekeeping gene *GAPDH* was used as a loading control.

stimulus (2.14), cellular catabolic process (1.53), transmembrane (1.33), ribonucleotide binding (1.3), RNA metabolic process (1.17), plasma membrane (0.93), protein modification (0.88), regulation of transcription (0.38). The upregulation of 10 clusters may coincide with cellular state transition of SKP spheres into SFC when cells acquire a strong potential of proliferation.

### Functional annotation clustering of downregulated genes

Of the 401 differentially expressed genes, 96 genes/clones were downregulated compared to the expression levels of SKP spheres ( $p \leq 0.05$ ) and 62 were successfully converted to DAVID IDs. The GO terms of downregulated genes are shown in Table 3. The featured GO terms are phosphoprotein and binding activity. One group was clustered with the enrichment score 0.67 (Fig. 4), including *zinc-finger domain proteins*, *bromodomain adjacent to zinc finger domain*, *pleiomorphic adenoma gene-like2*, *TATA box binding protein (TBP) associated factor*, *CGG triplet repeat binding protein*, and *CBP/p300 interacting transactivator*. These genes play a role in a broad range of transcriptional regulation. It seems that the downregulated zinc-finger proteins may be associated with the loss of neural potency during the transition of SKP spheres to SFC.

TABLE 1. GENE ONTOLOGY TERMS OF UPREGULATED GENES BETWEEN SKP AND SFC (COUNT  $\geq 10$ ,  $p$ -VALUE  $\leq 0.05$ )

<i>Term</i>	<i>Count</i>	<i>Percent (%)</i>	<i>p-Value</i>
Direct protein sequencing	56	29.8	7.4E-12
Acetylation	27	14.4	8.4E-12
Cytoplasm	95	50.5	2.0E-10
Intracellular part	122	64.9	1.0E-8
Ribonucleoprotein	16	8.5	1.7E-8
Ribosomal protein	14	7.4	3.6E-8
Cytoplasmic part	64	34.0	5.5E-8
Structural molecular activity	27	14.4	6.5E-8
Intracellular	125	66.5	6.6E-8
Macromolecular complex	50	26.6	1.8E-7
Ribosomal subunit	11	5.9	6.2E-7
Cellular biosynthetic process	29	15.4	1.1E-6
Structural constituent of ribosome	14	7.4	3.1E-6
Intracellular organelle part	57	30.3	3.4E-6
Translation	20	10.6	3.5E-6
Organelle part	57	30.3	3.8E-6
Intracellular organelle	103	54.8	3.9E-6
Organelle	103	54.8	4.0E-6
Biosynthetic process	33	17.6	4.2E-6
Intracellular nonmembrane-bound organelle	38	20.2	8.7E-6
Nonmembrane-bound organelle	38	20.2	8.7E-6
Ribosome	14	7.4	9.0E-6
Ribonucleoprotein complex	18	9.6	2.3E-5
Protein binding	89	47.3	3.2E-5
Mitochondrion	23	12.2	5.6E-5
Cytosol	16	8.5	8.5E-5
Phosphoprotein	63	33.5	8.9E-5
Protein complex	37	19.7	1.1E-5
Macromolecule biosynthetic process	21	11.2	1.9E-5
Protein dimerization activity	11	5.9	6.5E-4
Organelle lumen	20	10.6	8.0E-4
Membrane-enclosed lumen	20	10.6	8.0E-4
RNA binding	17	9.0	9.6E-4
Mitochondrial part	14	7.4	9.7E-4
Primary metabolic process	93	49.5	1.6E-3
Transit peptide	11	5.9	2.6E-3
Cytoskeleton	21	11.2	3.4E-3
Cell part	144	76.6	3.5E-3
Cell	144	76.6	3.6E-3
Localization	43	22.9	3.9E-3
Intracellular membrane-bound organelle	82	43.6	5.4E-3
Membrane-bound organelle	82	43.6	5.5E-3
Cellular metabolic process	90	47.9	7.0E-3
Nuclear part	19	10.1	7.6E-3
Organelle organization and biogenesis	20	10.6	1.1E-2
Cellular process	127	67.6	1.3E-2
Gene expression	46	24.5	1.3E-2
Binding	127	67.6	1.4E-2
Establishment of localization	36	19.1	2.1E-2
Transport	35	18.6	2.2E-2
Cell proliferation	14	7.4	2.7E-2
Nucleotide binding	21	11.2	2.9E-2
Cytoskeletal part	13	6.9	3.1E-2
Organelle envelope	11	5.9	3.1E-2
Envelop	11	5.9	3.2E-2
Protein metabolic process	44	23.4	3.3E-2
Regulation of cell proliferation	10	5.3	3.6E-2
Metabolic process	94	50.0	3.9E-2
Cellular macromolecule metabolic process	42	22.3	4.1E-2
Biological adhesion	13	6.9	4.6E-2
Cell adhesion	13	6.9	4.6E-2
Cytoskeleton organization and biogenesis	10	5.3	4.8E-2
Cellular protein metabolic process	41	21.8	5.0E-2

The "count" indicates the number of the genes involved in the term. The smaller  $p$ -value (EASE score) is, the more enriched (188 DAVID IDs).

TABLE 2. GENE FUNCTIONAL CLASSIFICATION OF UPREGULATED GENES IN SKF COMPARED WITH THOSE OF SKP SPHERES (10 CLUSTERS)

Functional cluster	Enrichment score	Genes
Cellular protein metabolic process	4.97	ribosomal protein sa, mitochondrial ribosomal protein l13, mitochondrial ribosomal protein l23, ribosomal protein l11, mitochondrial ribosomal protein s15, ribosomal protein s5, ribosomal protein l38, mitochondrial ribosomal protein s25, ribosomal protein l24, ribosomal protein l22, ribosomal protein l27, ribosomal protein s13, mitochondrial ribosomal protein l48, mitochondrial translational initiation factor 3, mitochondrial ribosomal protein l37
Nucleotide binding	2.49	sar1 gene homolog a ( <i>S. cerevisiae</i> ), heat-shock 70-kDa protein 8, tubulin, alpha, ubiquitous, eukaryotic translation elongation factor 1 alpha 1
Response to protein stimulus	2.14	heat-shock 60-kDa protein 1 (chaperonin), heat-shock 10 kDa protein 1 (chaperonin 10), heat-shock 70 kDa protein 8, heat-shock protein 90-kDa alpha (cytosolic), class a member 1
Cellular catabolic process	1.53	ubiquitin carboxyl-terminal esterase l1 (ubiquitin thiolesterase), proteasome (prosome, macropain) subunit, beta type, 6, proteasome (prosome, macropain) subunit, alpha type, 7, dcp1 decapping enzyme homolog a ( <i>S. cerevisiae</i> )
Transmembrane	1.33	bmp and activin membrane-bound inhibitor homolog ( <i>Xenopus laevis</i> ), solute carrier family 33 (acetyl-coa transporter), member 1, aquaporin 1 (colton blood group), tumor-associated calcium signal transducer 1
Ribonucleotide binding	1.3	dead (asp-glu-ala-asp) box polypeptide 18, heat-shock 70-kDa protein 8, mcm8 minichromosome maintenance deficient 8 ( <i>S. cerevisiae</i> ), dead (asp-glu-ala-asp) box polypeptide 55
RNA metabolic process	1.17	heterogeneous nuclear ribonucleoprotein h3 (2h9), heterogeneous nuclear ribonucleoprotein r, rod1 regulator of differentiation 1 ( <i>S. pombe</i> ), cleavage, and polyadenylation specific factor 3, 73 kDa
Plasma membrane	0.93	atpase, na + /k + transporting, beta 3 polypeptide, solute carrier family 33 (acetyl-coa transporter), member 1, solute carrier family 12 (potassium/chloride transporters), member 4, solute carrier family 23 (nucleobase transporters), member 2
Protein modification	0.88	casein kinase 1, alpha 1, v-mos moloney murine sarcoma viral oncogene homolog, discoidin domain receptor family, member 1, ptk9 protein tyrosine kinase 9
Regulation of transcription	0.38	sry (sex determining region y)-box 9 (campomelic dysplasia, autosomal sex-reversal), hypoxia-inducible factor 1, alpha subunit (basic helix-loop-helix transcription factor), mcm8 minichromosome maintenance deficient 8 ( <i>S. cerevisiae</i> ), taf5 rna polymerase ii, tata box binding protein (tbp)-associated factor, 100 kDa, nuclear factor (erythroid-derived 2)-like 1, nuclear factor (erythroid-derived 2)-like 2, pc4 and sfrs1 interacting protein 1, camp responsive element binding protein-like 2, chromosome 20 open reading frame 17, suppressor of ty 6 homolog ( <i>S. cerevisiae</i> ), rrn3 rna polymerase i transcription factor homolog (yeast), phd finger protein 23, ets homologous factor, nuclear factor of activated t-cells 5, tonicity-responsive, hypothetical protein bm-005, nuclear receptor subfamily 3, group c, member 1 (glucocorticoid receptor)

#### Differential pathways involved in upregulated and downregulated genes

The key signaling pathways were then identified in upregulated and downregulated gene lists. For upregulated genes, the potential enriched KEGG pathways are listed in Table 4. The highly involved pathways include cell communication, PPAR pathway, MAPK signaling pathway, Wnt signaling

pathway, ErbB signaling, ECM-receptor interaction, mTOR signaling pathway, and tumor growth factor (TGF)- $\beta$  signaling pathway. For downregulated genes, 5 BIOCARTA pathways were identified (Table 5): synaptic proteins in synaptic junction, Rac1 cell motility signaling pathway, role of Ran in mitotic spindle regulation, *Dicer* pathway, and mechanism of protein import into the nucleus. Thus, it appears that upregulated genes refer to extrinsic signaling pathways but

TABLE 3. GENE ONTOLOGY TERMS OF DOWNREGULATED GENES BETWEEN SKP AND SFC ( $P \leq 0.05$ )

Term	Count	Percent (%)	p-Value
Phosphoprotein	29	46.0	1.7E-4
Cytoplasm	19	30.0	4.7E-4
Intracellular	43	68.3	2.1E-3
Protein binding	33	52.4	2.8E-3
Oxidoreductase activity, acting on the CH-OH group of donors, NAD, or NADP as acceptor	4	6.3	4.7E-3
Oxidoreductase activity, acting on CH-OH group of donors	4	6.3	6.1E-3
Nucleus	24	38.1	7.0E-3
Intracellular part	40	63.5	7.9E-3
Intracellular membrane-bound organelle	32	50.8	8.7E-3
Membrane-bound organelle	32	50.8	8.8E-3
Intracellular organelle	35	55.6	1.1E-2
Organelle	35	55.6	1.1E-2
Nucleus	20	31.7	1.8E-2
Oxidoreductase activity	8	12.7	2.1E-2
Protein biosynthesis	4	6.3	2.4E-2
Regulation of apoptosis	6	9.5	2.4E-2
Regulation of programmed cell death	6	9.5	2.4E-2
Cytoskeleton	5	7.9	2.5E-2
Binding	46	73.0	3.3E-2
Positive regulation of apoptosis	4	6.3	4.3E-2
Nuclear part	8	12.7	4.3E-2
Positive regulation of programmed cell death	4	6.3	4.3E-2

The "count" indicates the number of the genes involved in the term (62 DAVID IDs).

downregulated genes for intrinsic cell function. The separate pathways involved in up- and downregulated genes manifest differential response of SKP cells to different extrinsic stimulus, which can be established and maintained by individual transcriptional states.

#### Real-time PCR for data validation

To verify the microarray data, we carried out real-time PCR by the relative standard curve method. We selected six genes: *COL1A2*, *RAN*, *ILKAP*, *NAP1L4*, *DCN*, and *PTGFR* (Tables 6). The real-time PCR data indicate a similar gene expression pattern with microarray data (Tables 7), confirming the reliability of our current microarray platform (Agca et al., 2006; Green et al., 2006; Whitworth et al., 2005).

#### Discussion

In this study we compared the transcriptional profiles of SKP spheres and SFC by microarray technology. Interestingly, the upregulated and downregulated genes are involved in differential extrinsic signaling and cell activities. The upregulated genes mainly relate to upstream signaling pathways that transduce external stimulus into downstream cellular responses; whereas the downregulated genes are involved in downstream cellular response such as transcriptional regulation, posttranscriptional modulation (noncoding RNA) and protein transportation. That is to say, the components of upstream signaling pathways are upregulated, whereas those of downstream cellular response pathways are

downregulated. Thus, it is suggested that SKP spheres and SFC may employ divergent signaling pathways in response to different extrinsic stimulus, reflecting the shift of stem cell state and fate *in vitro* (Enver et al., 2009).

It seems that the identified downregulated genes related pathways play a role in the regulation of stem cell identity. Initially, spectrin and ankyrin can build up the membrane skeleton of mammalian erythrocyte with other associated proteins. Their functions include targeting of ion channels and cell adhesion molecules to specialized compartment within the plasma membrane and endoplasmic reticulum of the nervous system, participation in epithelial morphogenesis, and orientation of mitotic spindles in asymmetric cell divisions (Bennett and Baines, 2001). Moreover, the Ran GTPase (Table 5), which is soluble, mobile, and concentrated by a nuclear import mechanism involving nuclear transport factor-2 (NTF2), can regulate the assembly of the mitotic spindle and the timing of cell-cycle transitions (Clarke and Zhang, 2008). Together it is tempting to speculate that Ran GTPase, NTF2, spectrin, and ankyrin may participate in the regulation of asymmetric cell division, which is a fundamental means of generating cell-fate diversity in the development of *Drosophila* nervous system (Jan and Jan, 2001). It is widely known that asymmetric cell division is a hallmark of stem cells, which enables them to simultaneously self-renewal and generate differentiated progeny (Knoblich, 2008), although asymmetric division is not necessary for stem cell identity but rather is a tool that stem cells can alternatively employ to maintain appropriate numbers of progeny either during development





TABLE 5. BIOCARTA PATHWAYS INVOLVED IN DOWNREGULATED GENES BETWEEN SKP SPHERES AND SFC

<i>BIOCARTA pathways</i>	<i>Involved genes</i>
Synaptic proteins at the synaptic junction	ankyrin 3, node of ranvier (ankyrin g); spectrin, beta, nonerythrocytic 1
Rac 1 cell motility signaling pathway	adp-ribosylation factor interacting protein 2 (arfaptin 2)
Role of Ran in mitotic spindle regulation	ran, member ras oncogene family
<i>Dicer</i> pathway	argonaute 4
Mechanism of protein import into the nucleus	nuclear transport factor 2

or during wound healing and regeneration (Morrison and Kimble, 2006). Nevertheless, asymmetric cell divisions promote stratification and differentiation of mammalian skin (Lechler and Fuchs, 2005). Therefore, we infer that asymmetric cell divisions are likely to be tuned up by the collaboration of Ran GTPase, spectrin, and ankyrin, which are suppressed in SFC cultures but promoted in SKP spheres (Table 3).

Another key pathway for downregulated genes is the *Dicer* pathway, implying a potential role of microRNAs (miRNAs) in the regulation of stem cell identity of SKP cells. *Dicer* catalyzes the first step in RNA interference (RNAi) and initiates the formation of RNA-induced silencing complex (RISC) whose catalytic component *Argonaute* family proteins can interact with miRNAs or small interfering RNAs (siRNAs) and function as a posttranscriptional regulator (Kim et al., 2009b). The miRNAs can serve as a key regulator in stem cells: regulating stem cell self-renewal and differentiation by suppression of specific target mRNA (Gangaraju and Lin, 2009). miRNAs are crucial for the regulation of self-renewal, cellular differentiation, and pluripotency in embryonic stem cells (Marson et al., 2008; Tay et al., 2008; Xu et al., 2009). In somatic stem cells, miR-124 regulates adult neurogenesis in the subventricular zone stem cell niche (Cheng et al., 2009), whereas miR-203 directly promotes epidermal differentiation in skin by restricting proliferation potential and inducing cell cycle exit (Yi et al., 2008). Most recently miR-145 and miR-143 have been demonstrated to regulate the smooth muscle cell fate and plasticity by multipotent stem cells (Cordes et al., 2009).

Furthermore, it was found that *Dicer* is required for the morphogenesis and maintenance of the hair follicle but is not essential for skin stem cell fate determination and differentiation (Andl et al., 2006; Yi et al., 2006). In addition, the pre-miRNAs are translocated into the cytoplasm by the exportin 5-Ran GTP shuttle system (Gangaraju and Lin, 2009). Thus, the downregulation of the Argonaute family may be correlated with the decreasing of the Ran family, resulting in less pre-miRNA present in the cytoplasm of SFC. Together, we infer that miRNA and/or asymmetric cell division may mediate the transition of stem cell state between SKP spheres and SFC.

The upregulated genes are mainly involved in extrinsic signaling pathways that transduce the external signaling into cellular parts, even though the stem cell behavior is regulated by both extrinsic signals and intrinsic programs (Li and Xie, 2005). During embryonic skin development, Wnt signaling blocks the ability of early ectodermal progenitor cell in response to FGFs, allowing them to respond to TGF-beta signaling and to adopt an epidermal fate (Fuchs, 2007). Wnt and TGF-beta signaling have substantial roles in the specification and activation of the hair follicle stem cells during embryonic skin development and adulthood (Blanpain and Fuchs, 2009): Wnt signaling can promote *de novo* hair follicle regeneration in adult skin after wounding (Ito et al., 2007) while cyclic dermal TGF-beta signaling regulates hair follicle stem cell activation during hair regeneration (Plikus et al., 2008). PPAR (peroxisome proliferator-activated receptor) signaling can induce and stimulate adipogenesis either in

TABLE 6. PRIMERS OF REAL-TIME QPCR USED FOR MICROARRAY DATA VALIDATION

<i>Clone ID/GenBank ID</i>	<i>Gene name</i>	<i>Primers</i>
UMC-pd12-14end-004-a01	<i>COL1A2</i>	Forward 5' GCACGATGCTCTGATCAATCCTTCTC 3' Reverse 5' GACGTTGGCCCAGTCTGTTTCAAAT 3'
pd12cl-016-c02	<i>PTGFR</i>	Forward 5' CACATGACACATTTACCTGCTGT 3' Reverse 5' TAGCTTACCTGTAGCACCGTCAT 3'
UMC-p4mm1-001-c03	<i>DCN</i>	Forward 5' AGAGCGCACATAGACACATCGGAA 3' Reverse 5' AACAAACAACATCTCTGCAGTCGGC 3'
UMC-pd3end3-009-a08	<i>RAN</i>	Forward 5' ACAACTGCTCTCCCGGATGAAGAT 3' Reverse 5' AAACACGCTGCAACCACTGACATC 3'
UMC-p4civp1-004-e01	<i>NAP1L4</i>	Forward 5' TACAAACGCATCGTGAGGAAGGCT 3' Reverse 5' GAGTGCCAGAGTTGCTTTACCCACA3'
UMC-pgvo2-009-c01	<i>ILKAP</i>	Forward 5' AGGACAAGATGAAGTGGACGGGT 3' Reverse 5' CCCAATGACAGGTTTATCTTGCTGGC 3'
AF017079	<i>GAPDH</i>	Forward 5' GCAAAGTGGACATTGTGCGCCATCA 3' Reverse 5' AGCTTCCCATTCTCAGCCTTGACT 3'

TABLE 7. RELATIVE GENE EXPRESSION LEVELS (MEAN  $\pm$  SEM AND *P*-VALUE) FROM MICROARRAY DATA AND REAL-TIME QPCR ANALYSIS

Genes	Microarray <sup>a</sup>			Real-time qPCR <sup>b</sup>		
	SKP	SFC	p-Value	SKP	SFC	p-Value
COL1A2	4.414 $\pm$ 1.517	1.727 $\pm$ 0.1946	0.0193	19.14 $\pm$ 1.636	13.15 $\pm$ 0.9843	0.02012
DCN	1.970 $\pm$ 0.2580	1.502 $\pm$ 0.09557	0.0971	36.10 $\pm$ 3.103	13.42 $\pm$ 0.8352	0.000406
RAN	1.289 $\pm$ 0.1502	0.9120 $\pm$ 0.05043	0.0284	17.07 $\pm$ 3.084	8.037 $\pm$ 0.4533	0.01586
NAP1L4	0.8591 $\pm$ 0.06463	0.5861 $\pm$ 0.07458	0.0293	1.705 $\pm$ 0.1433	1.212 $\pm$ 0.1447	0.03612
ILKAP	0.8525 $\pm$ 0.09328	0.5567 $\pm$ 0.08708	0.0471	0.5079 $\pm$ 0.03102	0.2440 $\pm$ 0.01712	2.2E-05
PTGFR	0.8448 $\pm$ 0.09936	1.471 $\pm$ 0.4090	0.0854	0.3916 $\pm$ 0.01005	0.8952 $\pm$ 0.1892	0.03764

<sup>a</sup>Microarray data were normalized to Ref cDNA.

<sup>b</sup>Real-time PCR values were normalized to house keeping gene *GAPDH*.

fibroblast or in mesenchymal stem cells (Hong et al., 2005; Lehrke and Lazar, 2005; Rosen et al., 1999). Recently it has been reported that PPAR signaling is required for maintaining a functional epithelial stem cell compartment of hair follicles (Harries and Paus, 2009; Karnik et al., 2009). In addition, activation of ERK/MAPK pathway often promotes cell division and is related with human cancers. Although Erk1/2 MAP kinase is required for normal epidermal G2/M progression (Dumesic et al., 2009), other MAPK-dependent signaling can also contribute to epithelial skin carcinogenesis (Bourcier et al., 2006), suggesting that the MAPK pathway has an important role in the control of skin epidermal proliferation (Fuchs, 2007). To sum up, Wnt, TGF- $\beta$ , PPAR, and MAPK signaling pathways mediate the proliferation, differentiation and cell fate determination in skin development and maintain the homeostasis in adult skin. We have detected upregulation of the components of these signaling pathways, showing their potential roles in controlling the growth and differentiation of SKP spheres *in vitro*.

In conclusion, we compared the transcriptional profiles between SKP spheres and SFC and identified potential signaling pathways conferring the molecular "stemness" of SKP spheres. The upregulated and downregulated genes are involved in extrinsic signaling pathways and intrinsic programs respectively, which could cooperate to choreograph the transcriptional state transition during the differentiation of SKP spheres to SFC. Our data pave the way for illustrating the molecular mechanisms of self-renewal and multipotency of skin derived stem cells, making it possible to take advantage of their potential therapeutic applications.

### Acknowledgments

We thank Dr. S. Clay Isom for helpful discussion, Kyle B. Dobbs for careful reading, and Dr. William G. Spollen at Department of Computer Science for cDNA library annotation. This work was supported by a grant from National Institutes of Health National Center for Research Resources (R01RR013438 to R.S.P.) and Food for the 21st Century at the University of Missouri.

### Author Disclosure Statement

The authors declare that no conflicting financial interests exist.

### References

- Agca, C., Ries, J.E., Kolath, S.J., et al. (2006). Luteinization of porcine preovulatory follicles leads to systematic changes in follicular gene expression. *Reproduction* 132, 133–145.
- Albert, M., and Peters, A.H. (2009). Genetic and epigenetic control of early mouse development. *Curr. Opin. Genet. Dev.* 19, 113–121.
- Andl, T., Murchison, E.P., Liu, F., et al. (2006). The miRNA-processing enzyme dicer is essential for the morphogenesis and maintenance of hair follicles. *Curr. Biol.* 16, 1041–1049.
- Arnold, S.J., and Robertson, E.J. (2009). Making a commitment: cell lineage allocation and axis patterning in the early mouse embryo. *Nat. Rev. Mol. Cell Biol.* 10, 91–103.
- Bartsch, G., Yoo, J.J., De Coppi, P., et al. (2005). Propagation, expansion, and multilineage differentiation of human somatic stem cells from dermal progenitors. *Stem Cells Dev.* 14, 337–348.
- Bennett, V., and Baines, A.J. (2001). Spectrin and ankyrin-based pathways: metazoan inventions for integrating cells into tissues. *Physiol. Rev.* 81, 1353–1392.
- Blanpain, C., and Fuchs, E. (2009). Epidermal homeostasis: a balancing act of stem cells in the skin. *Nat. Rev. Mol. Cell Biol.* 10, 207–217.
- Bourcier, C., Jacquelin, A., Hess, J., et al. p44 mitogen-activated protein kinase (extracellular signal-regulated kinase 1)-dependent signaling contributes to epithelial skin carcinogenesis. *Cancer Res.* 66, 2700–2707.
- Chambers, I., Silva, J., Colby, D., et al. (2007). Nanog safeguards pluripotency and mediates germline development. *Nature* 450, 1230–1234.
- Chen, F.G., Zhang, W.J., Bi, D., et al. (2007). Clonal analysis of nestin(–) vimentin(+) multipotent fibroblasts isolated from human dermis. *J. Cell Sci.* 120, 2875–2883.
- Cheng, L.C., Pastrana, E., Tavazoie, M., et al. (2009). miR-124 regulates adult neurogenesis in the subventricular zone stem cell niche. *Nat. Neurosci.* 12, 399–408.
- Clarke, P.R., and Zhang, C. (2008). Spatial and temporal coordination of mitosis by Ran GTPase. *Nat. Rev. Mol. Cell Biol.* 9, 464–477.
- Cordes, K.R., Sheehy, N.T., White, M.P., et al. (2009). miR-145 and miR-143 regulate smooth muscle cell fate and plasticity. *Nature* 460, 705–710.
- Crigler, L., Kazhanie, A., Yoon, T.J., et al. (2007). Isolation of a mesenchymal cell population from murine dermis that contains progenitors of multiple cell lineages. *FASEB J.* 21, 2050–2063.

- Dennis, G., Jr., Sherman, B.T., Hosack, D.A., et al. (2003). DAVID: database for annotation, visualization, and integrated discovery. *Genome Biol.* 4, P3.
- Dumesic, P.A., Scholl, F.A., Barragan, D.I., et al. (2009). Erk1/2 MAP kinases are required for epidermal G2/M progression. *J. Cell Biol.* 185, 409–422.
- Dyce, P.W., Zhu, H., Craig, J., et al. (2004). Stem cells with multilineage potential derived from porcine skin. *Biochem. Biophys. Res. Commun.* 316, 651–658.
- Enver, T., Pera, M., Peterson, C., et al. (2009). Stem cell states, fates, and the rules of attraction. *Cell Stem Cell* 4, 387–397.
- Fernandes, K.J., McKenzie, I.A., Mill, P., et al. (2004). A dermal niche for multipotent adult skin-derived precursor cells. *Nat. Cell Biol.* 6, 1082–1093.
- Fernandes, K.J., Toma, J.G., and Miller, F.D. (2008). Multipotent skin-derived precursors: adult neural crest-related precursors with therapeutic potential. *Philos. Trans. R. Soc. Lond. B Biol. Sci.* 363, 185–198.
- Fuchs, E. (2007). Scratching the surface of skin development. *Nature* 445, 834–842.
- Gangaraju, V.K., and Lin, H. (2009). MicroRNAs: key regulators of stem cells. *Nat. Rev. Mol. Cell Biol.* 10, 116–125.
- Green, J.A., Kim, J.G., Whitworth, K.M., et al. (2006). The use of microarrays to define functionally-related genes that are differentially expressed in the cycling pig uterus. *Soc. Reprod. Fertil. Suppl.* 62, 163–176.
- Harries, M.J., and Paus, R. (2009). Scarring alopecia and the PPAR-gamma connection. *J. Invest. Dermatol.* 129, 1066–1070.
- Hoheisel, J.D. (2006). Microarray technology: beyond transcript profiling and genotype analysis. *Nat. Rev. Genet.* 7, 200–210.
- Hong, J.H., Hwang, E.S., McManus, et al. (2005). TAZ, a transcriptional modulator of mesenchymal stem cell differentiation. *Science* 309, 1074–1078.
- Huang da, W., Sherman, B.T., and Lempicki, R.A. (2009). Systematic and integrative analysis of large gene lists using DAVID bioinformatics resources. *Nat. Protoc.* 4, 44–57.
- Ito, M., Yang, Z., Andl, T., et al. (2007). Wnt-dependent de novo hair follicle regeneration in adult mouse skin after wounding. *Nature* 447, 316–320.
- Ivanova, N.B., Dimos, J.T., Schaniel, C., et al. (2002). A stem cell molecular signature. *Science* 298, 601–604.
- Jan, Y.N., and Jan, L.Y. (2001). Asymmetric cell division in the *Drosophila* nervous system. *Nat. Rev. Neurosci.* 2, 772–779.
- Jiang, Y., Jahagirdar, B.N., Reinhardt, R.L., et al. (2002). Pluripotency of mesenchymal stem cells derived from adult marrow. *Nature* 418, 41–49.
- Joseph, N.M., and Morrison, S.J. (2005). Toward an understanding of the physiological function of Mammalian stem cells. *Dev. Cell* 9, 173–183.
- Karnik, P., Tekeste, Z., McCormick, T.S., et al. (2009). Hair follicle stem cell-specific PPARgamma deletion causes scarring alopecia. *J. Invest. Dermatol.* 129, 1243–1257.
- Kiel, M.J., Yilmaz, O.H., Iwashita, T., et al. (2005). SLAM family receptors distinguish hematopoietic stem and progenitor cells and reveal endothelial niches for stem cells. *Cell* 121, 1109–1121.
- Kim, D., Kim, C.H., Moon, J.I., et al. (2009a). Generation of human induced pluripotent stem cells by direct delivery of reprogramming proteins. *Cell Stem Cell* 4, 472–476.
- Kim, J., Lo, L., Dormand, E., et al. (2003). SOX10 maintains multipotency and inhibits neuronal differentiation of neural crest stem cells. *Neuron* 38, 17–31.
- Kim, V.N., Han, J., and Siomi, M.C. (2009b). Biogenesis of small RNAs in animals. *Nat. Rev. Mol. Cell Biol.* 10, 126–139.
- Knoblich, J.A. (2008). Mechanisms of asymmetric stem cell division. *Cell* 132, 583–597.
- Lechler, T., and Fuchs, E. (2005). Asymmetric cell divisions promote stratification and differentiation of mammalian skin. *Nature* 437, 275–280.
- Lehrke, M., and Lazar, M.A. (2005). The many faces of PPAR-gamma. *Cell* 123, 993–999.
- Li, L., and Xie, T. (2005). Stem cell niche: structure and function. *Annu. Rev. Cell Dev. Biol.* 21, 605–631.
- Lorenz, K., Sicker, M., Schmelzer, E., et al. (2008). Multilineage differentiation potential of human dermal skin-derived fibroblasts. *Exp. Dermatol.* 17, 925–932.
- Maisel, M., Herr, A., Milosevic, J., et al. (2007). Transcription profiling of adult and fetal human neuroprogenitors identifies divergent paths to maintain the neuroprogenitor cell state. *Stem Cells* 25, 1231–1240.
- Marson, A., Levine, S.S., Cole, M.F., et al. (2008). Connecting microRNA genes to the core transcriptional regulatory circuitry of embryonic stem cells. *Cell* 134, 521–533.
- Mitsui, K., Tokuzawa, Y., Itoh, H., et al. (2003). The homeoprotein Nanog is required for maintenance of pluripotency in mouse epiblast and ES cells. *Cell* 113, 631–642.
- Morrison, S.J., and Kimble, J. (2006). Asymmetric and symmetric stem-cell divisions in development and cancer. *Nature* 441, 1068–1074.
- Niwa, H., Burdon, T., Chambers, I., et al. (1998). Self-renewal of pluripotent embryonic stem cells is mediated via activation of STAT3. *Genes Dev.* 12, 2048–2060.
- Pittenger, M.F., Mackay, A.M., Beck, S.C., et al. (1999). Multilineage potential of adult human mesenchymal stem cells. *Science* 284, 143–147.
- Plikus, M.V., Mayer, J.A., de la Cruz, D., et al. (2008). Cyclic dermal BMP signalling regulates stem cell activation during hair regeneration. *Nature* 451, 340–344.
- Ramalho-Santos, M., Yoon, S., Matsuzaki, Y., et al. (2002). “Stemness”: transcriptional profiling of embryonic and adult stem cells. *Science* 298, 597–600.
- Rheinwald, J.G., and Green, H. (1975). Serial cultivation of strains of human epidermal keratinocytes: the formation of keratinizing colonies from single cells. *Cell* 6, 331–343.
- Rosen, E.D., Sarraf, P., Troy, A.E., et al. (1999). PPAR gamma is required for the differentiation of adipose tissue in vivo and in vitro. *Mol Cell* 4, 611–617.
- Sauka-Spengler, T., and Bronner-Fraser, M. (2008). A gene regulatory network orchestrates neural crest formation. *Nat. Rev. Mol. Cell Biol.* 9, 557–568.
- Shin, S., Sun, Y., Liu, Y., et al. (2007). Whole genome analysis of human neural stem cells derived from embryonic stem cells and stem and progenitor cells isolated from fetal tissue. *Stem Cells* 25, 1298–1306.
- Song, L., Webb, N.E., Song, Y., et al. (2006). Identification and functional analysis of candidate genes regulating mesenchymal stem cell self-renewal and multipotency. *Stem Cells* 24, 1707–1718.
- Takahashi, K., and Yamanaka, S. (2006). Induction of pluripotent stem cells from mouse embryonic and adult fibroblast cultures by defined factors. *Cell* 126, 663–676.
- Tay, Y., Zhang, J., Thomson, A.M., et al. (2008). MicroRNAs to Nanog, Oct4 and Sox2 coding regions modulate embryonic stem cell differentiation. *Nature* 455, 1124–1128.
- Terada, N., Hamazaki, T., Oka, M., et al. (2002). Bone marrow cells adopt the phenotype of other cells by spontaneous cell fusion. *Nature* 416, 542–545.

- Terskikh, A.V., Miyamoto, T., Chang, C., et al. (2003). Gene expression analysis of purified hematopoietic stem cells and committed progenitors. *Blood* 102, 94–101.
- Toma, J.G., Akhavan, M., Fernandes, K.J., et al. (2001). Isolation of multipotent adult stem cells from the dermis of mammalian skin. *Nat. Cell Biol.* 3, 778–784.
- Toma, J.G., McKenzie, I.A., Bagli, D., et al. (2005). Isolation and characterization of multipotent skin-derived precursors from human skin. *Stem Cells* 23, 727–737.
- Tumbar, T., Guasch, G., Greco, V., et al. (2004). Defining the epithelial stem cell niche in skin. *Science* 303, 359–363.
- Wagers, A.J., and Weissman, I.L. (2004). Plasticity of adult stem cells. *Cell* 116, 639–648.
- Wagner, W., Wein, F., Seckinger, A., et al. (2005). Comparative characteristics of mesenchymal stem cells from human bone marrow, adipose tissue, and umbilical cord blood. *Exp. Hematol.* 33, 1402–1416.
- Whitworth, K., Springer, G.K., Forrester, L.J., et al. (2004). Developmental expression of 2489 gene clusters during pig embryogenesis: an expressed sequence tag project. *Biol. Reprod.* 71, 1230–1243.
- Whitworth, K.M., Agca, C., Kim, J.G., et al. (2005). Transcriptional profiling of pig embryogenesis by using a 15-K member unigene set specific for pig reproductive tissues and embryos. *Biol. Reprod.* 72, 1437–1451.
- Whitworth, K.M., Li, R., Spate, L.D., et al. (2009). Method of oocyte activation affects cloning efficiency in pigs. *Mol. Reprod. Dev.* 76, 490–500.
- Xu, N., Papagiannakopoulos, T., Pan, G., et al. (2009). MicroRNA-145 regulates OCT4, SOX2, and KLF4 and represses pluripotency in human embryonic stem cells. *Cell* 137, 647–658.
- Yi, R., O'Carroll, D., Pasolli, H.A., et al. (2006). Morphogenesis in skin is governed by discrete sets of differentially expressed microRNAs. *Nat. Genet.* 38, 356–362.
- Yi, R., Poy, M.N., Stoffel, M., et al. (2008). A skin microRNA promotes differentiation by repressing "stemness." *Nature* 452, 225–229.
- Ying, Q.L., Nichols, J., Evans, E.P., et al. (2002). Changing potency by spontaneous fusion. *Nature* 416, 545–548.
- Zhao, M., Isom, S.C., Lin, H., et al. (2009). Tracing the stemness of porcine skin-derived progenitors (pSKP) back to specific marker gene expression. *Cloning Stem Cells* 11, 111–122.
- Zhou, H., Wu, S., Joo, J.Y., et al. (2009). Generation of induced pluripotent stem cells using recombinant proteins. *Cell Stem Cell* 4, 381–384.

Address correspondence to:  
*Dr. Randall S. Prather*  
*Division of Animal Sciences*  
*University of Missouri*  
*920 East Campus Drive*  
*Columbia, MO 65211*

*E-mail: PratherR@missouri.edu*

